Check for updates

Development and performance optimization of a new composite sealing material prepared by drilling cuttings

Xiaoping Li[1], Guoping Han[1], Yong Wang[1], Jie Xu[1], Jie Du[1], Bo Yang[1], Min Zhang[1], Tao Li[1], Bo Li[2]* and Junxiang Zhang[3]

[1]Tunlan Mine, Shanxi Coking Coal Group Co., Ltd., Gujiao, China, [2]School of Safety Science and Engineering, Henan Polytechnic University, Jiaozuo, Henan, China, [3]School of Energy and Environment Engineering, Zhongyuan University of Technology, Zhengzhou, Henan, China

A highly efficient composite sealing material was prepared using drilling cuttings as the base material and a binder, a coagulant, and other additives as auxiliaries. A four-factor, three-level orthogonal test was designed based on the response surface method (RSM), and a response surface regression model was constructed using compressive strength, fluidity, expansion rate, and setting time as performance indexes to analyze the effects of each factor on material performance and optimize the material proportion. The samples were prepared by simulating the grouting process, the permeability of the samples was measured, and the sealability of the material was verified by analyzing the material microscopic morphology. Results showed that the regression model had a high level of confidence and accuracy and could predict the test results accurately within the range of the test. The effects of the interaction between factors on material performance were also examined. The low permeability of the sealing material samples verified the material's feasibility. Gradual optimization of material performance revealed that the optimal proportion was 52.6% drill cuttings, 44.3% binder, 0.6% coagulant promoter, and 2.5% expansive agent. Under these conditions, the error between the predicted and test values of each material property was less than 5%, and the comprehensive performance was superior. These findings verify the accuracy of RSM and its applicability to the optimization of material performance. This work provides reasonable theoretical guidance for the preparation of drilling cuttings composite (DC) materials in practical engineering.

KEYWORDS

response surface methodology, drilling cuttings, sealing material, analysis of variance, performance optimization

1 Introduction

With the intensive development of China's coal industry, the gas storage conditions in deep coal seams have become complicated and variable, and coal and gas protrusion disasters are becoming increasingly frequent (Xie, 2019). Gas extraction is a fundamental measure to control coal and gas protrusion because it can quickly reduce the gas content and gas pressure and utilize the extracted gas as clean energy (Xiong, 2020; Yan and Chen, 2021). Borehole grouting sealing is a key technology for gas extraction, and the physical and chemical properties of the sealing material directly affect the quality of drilling sealing (Xue et al., 2020; Zuo et al., 2022). Therefore, research on the optimization of sealing materials'

performance and regulation mechanism is an important basic guarantee for the efficient extraction of coal seam gas.

Existing sealing materials can be divided into two categories: inorganic and organic. Inorganic sealing materials are divided into cementitious, clay mineral, and high-water-content materials (Martin et al., 2019; Wang et al., 2022). Cementitious materials are inexpensive, easy to obtain, and entail a simple process, but they also have defects, such as long setting time, water loss, contraction that produces fractures that result in sealing leakage, and difficulty in meeting the sealability requirements of boreholes (Li et al., 2019a; Liu S. et al., 2023a; Liu and Li, 2023). Clay mineral materials include yellow clays, which are not conducive to deep hole sealing because of their high viscosity that leads to low slurry flow and difficulty in penetrating and diffusing effectively around the borehole (Bai et al., 2021; Fu et al., 2021). High-water-content materials have the advantages of high water–cement ratio flowability, microexpansion, high toughness (can maintain good mechanical properties under the action of drilling force), and good sealing compactness. The disadvantages are that the setting time is long, strength development is slow, and early concretion strength is difficult to ensure. The negative pressure around the borehole and the external forces within the concretion easily produce new fractures, resulting in poor sealing of the borehole (Ni et al., 2020; Wang, 2021). Commonly used organic materials include polyurethane and Marisan. Polyurethane generally has a high curing speed, a high expansion rate, and strong adhesion, and its concretion has good strength and toughness (Zhang et al., 2019). However, the extremely high foaming speed of polyurethane cannot be controlled, and the problem of high viscosity makes sealing the borehole wall difficult, resulting in the formation of leakage between the borehole wall and the concretion (Li et al., 2023; Zhang et al., 2023). In addition, polyurethane is a toxic polymer material, and using a large amount of it causes environmental pollution, which is not conducive to the development needs of green mines. Marisan is a polyimide resin and catalyst adhesive. It has good sealing performance and is widely used in the "twice plugging and one injection" sealing process and in determining gas pressure in coal seams (Bai et al., 2019). However, its high price and toxicity limit its widespread use.

Drilling cuttings from drilling construction are a kind of coal gangue solid waste, they are discharged to the workplace and occupy the limited space. If not treated in time, they will block the mine ventilation and contaminate the underground working environment, thereby seriously jeopardizing the health of underground personnel (Liu H. et al., 2023b). The use of drilling cuttings and additives to prepare sealing materials is an important means of dealing with underground waste, using coal cleanly to achieve waste recycling and zero discharge, and reducing underground environmental pollution (Zhang and Zhai, 2019).

In view of these deficiencies in existing sealing materials, this study prepared a kind of DC material with other additives (binders, coagulants, etc.) as auxiliary materials. A four-factor, three-level orthogonal test was designed using the Box–Behnken module of Design Expert software. The regression model between the factors and response values was established with compressive strength, fluidity, setting time, and expansion rate as performance indexes. ANOVA and the response surface method (RSM) were used to analyze the law of the influence of each factor on material performance. The orthogonal test results were utilized to verify the accuracy and applicability of the regression model, establish a regulation mechanism for optimizing the performance of DC materials, and meet the technological needs of grouting and sealing.

2 Test preparation

2.1 Raw material

The drilling cuttings used in the test were made up of anthracite, and the coal samples were crushed into samples with a particle size of less than 1 mm. The binder used in the composite material was water-soluble resin, which underwent polymerization under the action of a coagulant to form a 3D network polymer and could simultaneously encapsulate the drilling cutting particles to form a continuous structural whole (Yan and Chen, 2021). The coagulant was a weak acid salt that is easily soluble in water, nontoxic, and nonpolluting (Chen et al., 2022). The aqueous solution was weakly acidic and could accelerate the polymerization of the binder molecule. The expansive agent was an inorganic carbonate that absorbs heat and decomposes to produce CO_2 or reacts with hydrogen ions in the material to produce CO_2, thereby promoting the expansion of the composite material while reducing the heat released by the material reaction.

2.2 Test methods

An orthogonal test was conducted on the DC material by using compressive strength, fluidity, setting time, and expansion rate as the performance indexes. The determination methods for the index parameters were as follows:

(1) The compressive strength test employed the RMT-150B rock mechanics experimental system. After the composite material reached the setting time, the demolded material was cut into standard specimens with a diameter of 50 mm and a height of 100 mm by using a cutting machine in accordance with DZT0276.20-2015 (Test Procedure for Physical and Mechanical Properties of Rocks).

(2) The fluidity test employed a cement sand flow tester, and the composite material slurry was stirred evenly until the completion time of the measurement (controlled within 5 min).

(3) The setting time test used the standard Vickers apparatus and was based on GB1346-2001 (Test Methods for Water Requirement of Normal Consistency, Setting Time and Soundness of Portland Cement).

(4) The expansion rate was tested by the drainage method, and the testing apparatus included electronic scales, paraffin, and plastic beakers. First, the prepared material slurry was poured into a plastic beaker of volume V_0. After the material had fully expanded and solidified, it was removed from the beaker and weighed using an electronic scale. Its mass was recorded as m_1. Second, the surface of the material was evenly coated with paraffin, and an electronic scale was used to weigh its mass, which was marked as m_2. The mass of paraffin coated on the surface of the material was the difference between the two weighed masses, that is, $\Delta m = m_2 - m_1$. The density of paraffin was utilized to calculate the volume of the paraffin coating (V_1). Last, the paraffin-coated material was placed in water, and its volume was measured as V_2. The expansion volume of the material after solidification was $V_2 - V_1 - V_0$. The expansion rate of the material was obtained with Eq. 1.

TABLE 1 Experimental protocol and results.

Experiment number	Factors				Experiment results			
	A/g	B/g	C/g	D/g	Y_1/MPa	Y_2/mm	Y_3/min	Y_4/%
1	90	70	0.8	2.5	6	241	90	9.8
2	110	70	1	5	7.5	217	45	11
3	90	80	1.2	7.5	10.42	215	47	13.6
4	110	80	1	5	6.7	208	64.4	7.5
5	100	75	0.8	2.5	10.3	220.1	90	8.6
6	100	75	1.2	2.5	9	222	49	9.5
7	100	75	0.8	7.5	7.3	218	78	15.4
8	100	75	1.2	7.5	7.7	218	55	12.5
9	90	75	0.8	5	8.1	236	88	10.8
10	110	75	1	2.5	8.3	220	56	7
11	90	75	1	7.5	7.6	228.5	63	12.1
12	110	75	1	7.5	6.8	209	57.5	13
13	100	70	0.8	5	6.7	224	77.5	12.5
14	100	80	0.8	5	7.9	215	84	13.5
15	100	70	1.2	5	6.1	223	41	13.2
16	100	80	1.2	5	9.5	213	60	8.3
17	90	75	1	5	9.5	230	68	13.5
18	110	75	0.8	5	7.7	211	71	16
19	90	80	1	5	11.8	221	56	11.5
20	110	75	1.2	5	7.8	216	49	6
21	100	70	1	2.5	7.3	226	52	14
22	100	80	1	2.5	9.5	214	74	5.6
23	100	70	1	7.5	6.2	224.4	59	13
24	100	80	1	7.5	8.5	210	74	16
25	100	75	1	5	10.2	220	63.6	13.1
26	100	75	1	5	9.7	223	60	12.6

$$\eta = \frac{V_2 - V_1 - V_0}{V_0} \times 100\% \qquad (1)$$

Where V_0 is the volume of the plastic beaker, V_1 is the volume of the paraffin coating, and V_2 is the volume of the paraffin coated material, m³; η is the expansion rate of the material.

2.3 Experiment design

Orthogonal tests were conducted with drilling cuttings (A), binder (B), coagulant (C), and expansive agent (D) as the four main factors, and three levels were selected for each factor. The level of factor A was set to 90 and 110 g, the level of factor B was set to 70 and 80 g, the level of factor C was set to 0.8 and 1.2 g, and the level of factor D was set to 2.5 and 7.5 g. Compressive strength (Y_1), fluidity (Y_2), setting time (Y_3),

and expansion ratio (Y_4) were used as performance indexes. Design Expert 11.0 was employed to design a three-factor, four-level orthogonal experimental protocol with a total of 26 sets of proportioning schemes. The abovementioned index test method was used to test the performance of the material under the conditions of each proportion, and the orthogonal test results are shown in Table 1.

3 Experimental results and analysis

3.1 Analysis of model fitting accuracy

On the basis of the results of the orthogonal test shown in Table 1, the influencing factors for each indicator were fitted to obtain quadratic multiple-regression equations, which are shown in

TABLE 2 Regression model ANOVA.

Sources	Compressive strength (Y_1)		Fluidity (Y_2)		Setting time (Y_3)		Expansion ratio (Y_4)	
	F	p	F	p	F	p	F	p
Model	17.67	<0.0001**	35.38	<0.0001**	24.19	<0.0001**	18.18	<0.0001**
A	14.48	0.0029**	181.87	<0.0001**	5.40	0.0502	15.90	0.0021**
B	77.03	<0.0001**	125.84	<0.0001**	32.52	0.0001**	21.83	0.0007**
C	0.4475	0.5173	1.40	0.2617	186.55	<0.0001**	14.22	0.0031**
D	38.42	<0.0001**	15.44	0.0024**	0.0067	0.9363	60.39	<0.0001**
AB	49.55	<0.0001**	3.94	0.0726	7.69	0.0181*	0.3429	0.5700
AC	0.6032	0.4537	16.06	0.0021**	6.20	0.0300*	44.18	<0.0001**
AD	1.08	0.3200	5.02	0.0567	0.1168	0.7390	9.13	0.0116*
BC	7.55	0.0190*	0.0010	0.9752	2.23	0.1631	12.26	0.0050**
BD	0.1521	0.7040	0.1500	0.7059	1.48	0.2495	44.18	<0.0001**
CD	4.78	0.0513	0.0565	0.8166	5.10	0.0452*	5.15	0.0544
A^2	14.34	0.0030**	3.92	0.0731	7.07	0.0222*	6.68	0.0254*
B^2	40.19	<0.0001**	4.08	0.0685	1.26	0.2859	2.43	0.1473
C^2	14.22	0.0031**	0.2965	0.5969	3.53	0.0869	0.9175	0.3587
D^2	8.24	0.0152*	0.6431	0.4396	0.5616	0.4693	3.63	0.0834
R^2	0.9574		0.9583		0.9185		0.9486	
R^2_{adj}	0.9033		0.9506		0.9285		0.9059	
R^2_{pred}	0.7592		0.8714		0.8492		0.7273	

"*" represents significant ($p < 0.05$); "**" indicates extremely significant ($p < 0.01$).

Eqs 2–5. The regression equations were calculated to obtain the results of the variance of each indicator, as shown in Table 2. The ANOVA results showed that the p-value of each model term is 0.0001, which is less than 0.01, indicating that the relationship between the response values (Y_1, Y_2, Y_3, and Y_4) and the regression equation is highly significant, and the credibility of the regression equation is high. Meanwhile, the coefficients of determination (R^2) of the response values are 0.9574, 0.9583, 0.9185, and 0.9486, which are close to 1, indicating that the accuracy of the model fit is high. The difference between R^2_{adj} and R^2_{pred} of each response value is less than 0.2, which indicates that the error between the response value and the real value is small and further confirms that the regression equation has high fitting accuracy. The quadratic multiple regression equation can truly reflect the relationship between the response value and the influence of the factors.

$$Y_1 = 9.81 - 0.61A + 1.24B + 0.10C - 0.87D - 1.84AB - 0.21AC + 0.27AD + 0.61BC + 0.09BD + 0.49CD - 0.84A^2 - 1.31B^2 - 0.77C^2 - 0.59D^2 \tag{2}$$

$$Y_2 = 220.81 + 8.09A - 5.93B - 0.64C - 2.08D + 1.94AB + 4.14AC - 2.19AD + 0.03BC - 0.32BD - 0.20CD + 1.65A^2 - 1.57B^2 - 0.42C^2 - 0.62D^2 \tag{3}$$

$$Y_3 = 64.09 - 3A + 6.49B - 15.89C + 0.09D + 5.85AB + 5.54AC + 0.72AD + 2.69BC - 2.19BD + 4.06CD - 4.76A^2 - 1.87B^2 + 3.1C^2 + 1.25D^2 \tag{4}$$

$$Y_4 = 12.98 - 1.22A - 1.26B - 1.04C + 2.1D - 0.29AB - 3.51AC + 1.51AD - 1.49BC + 2.83BD - 0.97CD - 1.1A^2 - 0.62B^2 - 0.37C^2 - 0.75D^2 \tag{5}$$

3.2 Relationship between response values and influencing factors

3.2.1 Analysis of factors that affect compressive strength

The stress condition around a borehole is complex and remains unsupported for a long time after construction, so the borehole is prone to damage during gas extraction and sealing operations. In addition, under the negative pressure of gas extraction and coal mining, if the strength of the sealing material is too low, secondary cracks will occur, making it difficult to seal the gas leakage channel (Zhu et al., 2021; Jing et al., 2022). Therefore, the sealing material needs to have a certain early strength to achieve timely support for the borehole, thus preventing the occurrence of unstable deformation during drilling that results in the formation of air leakage rings (Guo et al., 2022; Wei et al., 2022).

Through the analysis of the orthogonal experiment, ANOVA was performed on the effect of various factors on compressive strength, as shown in Table 2. The p-value of compressive strength in Table 2

indicates that A, B, and D are all highly significant. The F value shows that the degree of influence of each significant factor on compressive strength is in the order of $B > D > A$, with B having the greatest influence. Coal is a natural polymer organic mineral, and its molecular structure consists of aromatic hydrocarbons with different degrees of condensation and bridging bonds connected to the aromatic ring (Xiong et al., 2021). This structure gives the coal molecules a certain rigidity and allows them to be used as rigid particles in polymers. The resin binder polymerizes under the action of the coagulant to form a high-strength composite matrix. Therefore, the influence of factor B on the compressive strength of materials is significant.

3.2.2 Analysis of factors that affect fluidity

The composite sealing material should have good fluidity to ensure that the slurry can flow into the fractures around the borehole to the maximum extent under grouting pressure and to seal the fractures to the maximum extent. The p-value from the ANOVA of mobility in Table 2 shows that A, B, and D are all highly significant. The F value indicates that the degree of influence of each factor on mobility is in the order of $A > B > D$. The reason is that the surface of drilling cutting particles is rough, and an excessive particle content increases the internal frictional force of the composite. This condition increases the internal viscous resistance of the slurry during the flow process, resulting in a decrease in the fluidity of the slurry. Therefore, factor A has the greatest influence on fluidity.

3.2.3 Analysis of factors that affect setting time

Setting time is an important indicator of sealing materials and directly determines the design of the sealing process (Li et al., 2019b). The slurry setting time should not be too low nor too high, and the slurry must be mixed in the laboratory in advance in accordance with the actual project conditions (Li et al., 2022). An appropriate setting time prevents the slurry from solidifying prematurely during the flow process and ensures that the slurry spreads sufficiently around the borehole to achieve the desired blocking effect (Zheng et al., 2021). The analysis of the p values from the variance of setting time in Table 2 shows that B and C are highly significant. The F value indicates that the degree of influence of each factor on the setting time of the material is in the order of $C > B$, with factor C having the greatest influence. The main reason is that the coagulant can produce a certain amount of free radicals in the slurry, which triggers the polymerization of the resin molecules. Increasing the coagulant dosage accelerates the intermolecular bonding rate, thus reducing the setting time of the materials. In accordance with the actual sealing process demand, the material setting time should be controlled within 30–60 min, so factor C mixing should be controlled within the appropriate range.

3.2.4 Analysis of factors that affect the expansion rate

According to the principle of action and reaction forces, the expansion that occurs in the volume of the slurry after solidification can provide support for the borehole wall. At the same time, it can compress the loose area of the borehole wall and further compress the fracture. Therefore, the expansion of the sealing material is important to improve the sealing effect. The p-value from the ANOVA of the expansion rate in Table 2 shows

that A, B, C, and D are highly significant. The F value indicates that the degree of influence of each factor on the expansion rate of the material is in the order of $D > B > A > C$. Factor D has the greatest influence. The main reason is that the expansive agent reacts with the hydrogen ions provided by the water in the material to produce gas, which causes internal expansion of the material. The more expansive the added agent is, the more obvious the expansion effect is.

3.3 Response surface analysis

Through the response surface models, the performance of the DC material was visualized. Such performance is affected not only by the action of a single factor, but also by the interaction of several factors. According to Table 2, the effect of AB and BC interactions on the compressive strength of the material is significant, and according to the F value, the magnitude of the effect of AB is greater than that of BC. This result indicates that the AB interaction term has the greatest influence on compressive strength. Figure 1A shows that the compressive strength of the material increases and then decreases with binder dosage at each fixed value of 90–100 g of drilling cutting proportion. Extreme values of drilling cuttings and binder dosage were observed, and they optimized the compressive strength, which reached its maximum value at 90 g of drilling cuttings and 80 g of the binder.

According to Table 2, the effect of AC interaction on material fluidity is highly significant and the largest. Figure 1B shows that when the coagulant dosage is 0.8–1.2 g, material fluidity increases with the decrease in the proportion of drilling cuttings, and it reaches the maximum value when the curing agent is 0.8 g and the amount of drilling cuttings is 90 g.

According to Table 2, the effects of AB, AC, and CD interactions on material setting time are significant. The F value indicates that the degree of influence from the largest to the smallest is AC, AB, and CD, the AC interaction has the greatest influence on setting time. As shown in Figure 1C, when the dosage of drilling cuttings is 90–110 g, the fluidity of the material increases as the proportion of drilling cuttings decreases, and the setting time reaches the maximum value when the coagulant is 0.8 g and the amount of drilling cuttings is 90 g.

According to Table 2, the effects of AC, BC, and BD interactions on the material expansion rate are significant. The F value shows that the degree of influence from the largest to the smallest is BD, AC, and BC, the AC interaction has the greatest influence on the expansion rate. Figure 1D indicates that when the binder dosage is 70–80 g, the material expansion rate increases as the proportion of drilling cuttings decreases. When the expansive agent is greater than 5.5 g, the expansion rate decreases with the increase in the expansive agent's dosage. The maximum expansion rate was obtained when the expansive agent is 7.5 g and the binder is 80 g.

3.4 Comparison of actual and predicted values

We drew (x, y) scatter plots on the basis of the measured values of the experimental results and model prediction data. The actual and predicted values of compressive strength (Y_1), fluidity (Y_2),
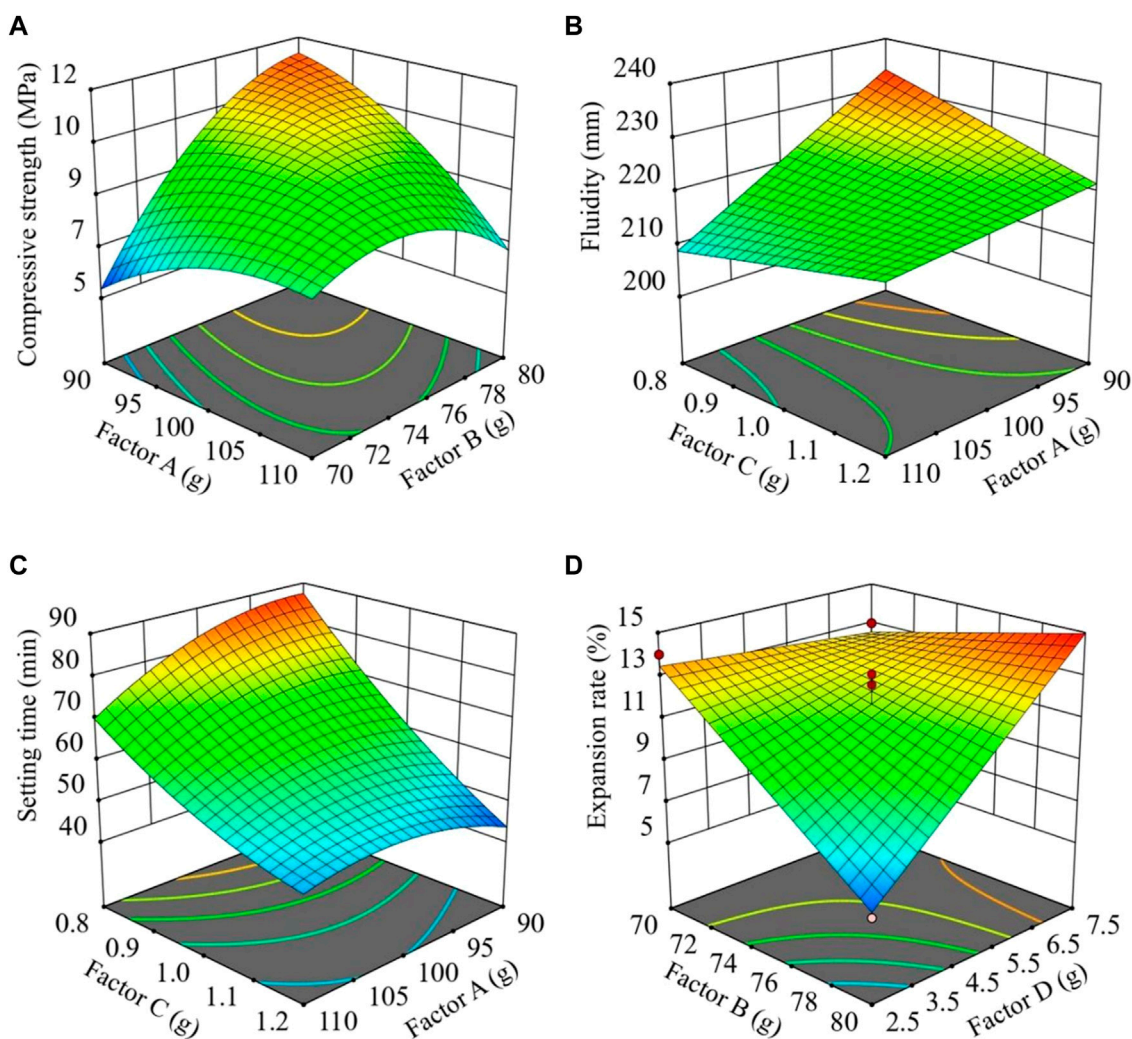
FIGURE 1
Surface plot of the effect of *BD* synergy term on expansion rate. **(A)** AB interaction on the compressive strength. **(B)** AC interaction on the fluidity. **(C)** AC interaction on the setting time. **(D)** BD interaction on the expansion rate.

setting time (Y_3), and expansion rate (Y_4) were compared. The comparative analysis is shown in (Figures 2A–D). The scatter points are distributed on a straight line and located near the diagonal, indicating the high accuracy of model fitting. Therefore, the model regression equations (Eqs 2–5) can be used to optimize and predict the compressive strength, fluidity, setting time, and expansion rate of this composite sealing material, which corroborates the previous analysis.

4 Analysis of composite material sealing characteristics

4.1 Grouting sealing simulation test

4.1.1 Testing process
4.1.1.1 Experimental material selection
The experimental equipment included a pressurized pump, a pressure-retaining device, a self-sealing bag, and a connecting pipe.

The test materials included polyurethane, superfine cement, and DC materials.

4.1.1.2 Sample preparation
Large coal briquettes were made into cylindrical samples of 50 mm × 100 mm by using a coal sample drilling machine and a cutting mill, and the permeability of the coal samples was tested with a three-axis seepage test system. The cylindrical coal samples with heat-shrinkable tubes were fixed on the gripper of the drilling machine, and the drilling machine was utilized to create boreholes with a diameter of 5 mm through the upper and lower circular surfaces of the cylindrical specimens.

4.1.1.3 Experimental procedures
The prepared cement, DC material, and coal samples were placed in the self-sealing bag. After removing the air from the self-sealing bag, the bag was sealed. The self-sealing bag was then placed in a pressure-retaining container filled with water, pressurized to 1 MPa by using a pressure pump, and removed
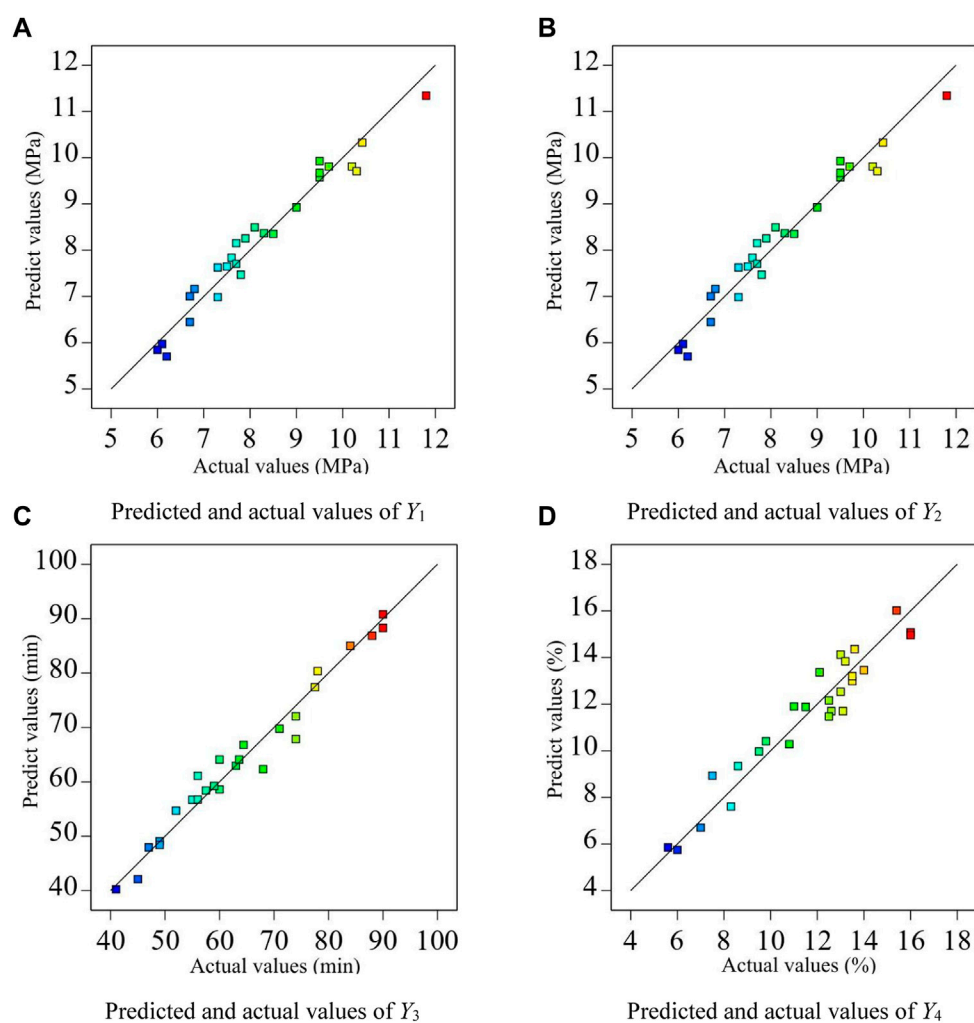
FIGURE 2
Predicted and actual values of response values.

after 6 h of pressure retention. The polyurethane sealing material was tucked in by using a coiling method. Three days after the end of the experiment, the coal samples were cleaned of the surface sealing material, and the samples were tested for permeability. The experimental system is shown in Figure 3, and the test samples are presented in Figure 4.

4.1.2 Test results

Samples 1, 2, and 3 were sealed with the cement slurry sealing material, Samples 4, 5, and 6 were sealed with the polyurethane sealing material, and Samples 7, 8, and 9 were sealed with the DC material. During the permeability test, the axial load, confining pressures, and air pressure were set to 1, 1, and 0.23 MPa, respectively. The permeability test results are shown in Figure 5.

As shown in Figure 5, the permeability of the coal samples sealed with the three different sealing materials increased at different degrees. The smallest increase was observed in Samples 7, 8 and 9, followed by Samples 1, 2, and 3. The largest increase was found in Samples 4, 5, and 6. The samples with the DC material had the

lowest permeability, followed by the samples with cement slurry and polyurethane sealing material.

4.2 Microscopic morphology analysis

On the basis of the grouting simulation experiment, the microscopic morphology of the contact surface between the three sealing materials and coal was analyzed to further verify the sealing materials' performance. The test samples were selected from the contact part between the grouting material and the borehole wall, and their dimensions were 1 cm × 1 cm × 0.5 cm. The test samples were vacuum sprayed with gold, and the scanning electron microscope results are shown in Figure 6.

As shown in Figure 6A, magnification of the cement slurry sample by 400 times showed that the fracture on the cemented surface is smaller than that in the polyurethane-sealed sample, but its permeability is higher. The cement particles cannot easily enter the small fracture, resulting in poor sealing. As shown in Figure 6B, a large fracture can be found between polyurethane and coal when the
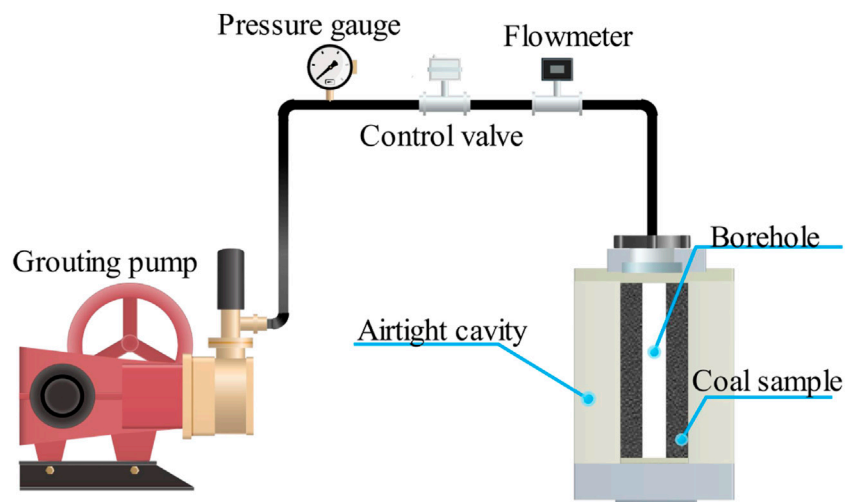
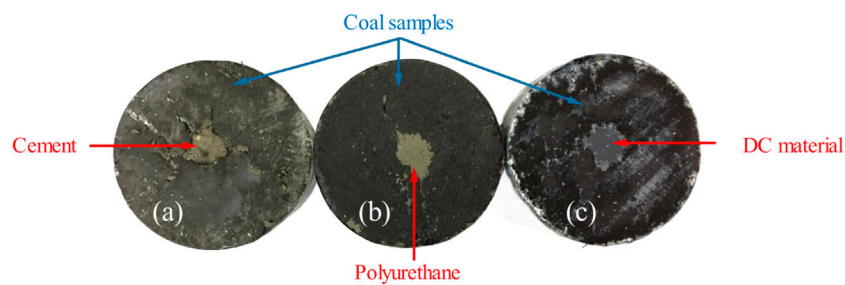**FIGURE 3**
Schematic diagram of experimental system.

FIGURE 4
Test samples: **(A)** cement, **(B)** polyurethane, **(C)** DC material.
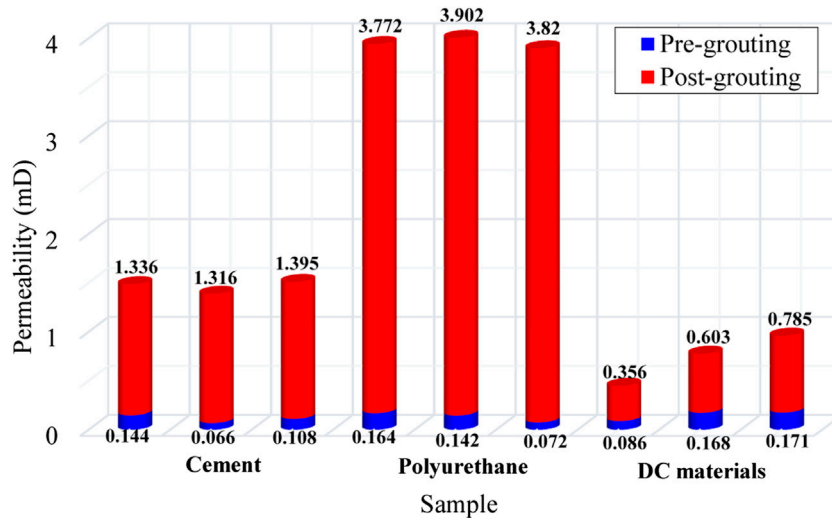

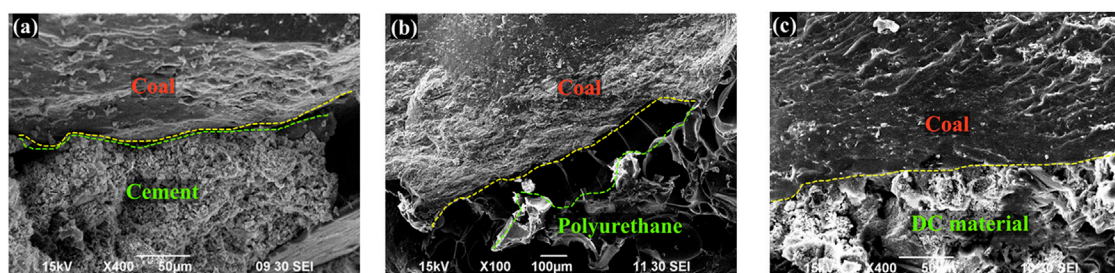**FIGURE 5**
The permeability of samples.

FIGURE 6
Microstructure of sealing material.

sample sealed with polyurethane is magnified by 100 times, indicating that the bonding between polyurethane and coal at the hole wall is loose. Polyurethane foams quickly, its viscosity increases rapidly, fluidity attenuation is blocked, and the material cannot easily enter the surrounding fracture. In addition, many impurities are attached to the surface of the borehole wall and result in poor contact between polyurethane and coal at the borehole wall, ultimately leading to poor sealing. As shown in Figure 6C, magnification of the DC material by 400 times revealed that the contact surface is seamless, indicating close contact on the contact surface. The sealing material contains water-soluble components that can enter the tiny fracture on the borehole wall under the action of grouting pressure, making the coal and the components in the sealing material combine tightly to improve the quality of borehole sealing.

4.3 Discussion

The discussion of the interaction factors above showed that the maximum performance of the DC material in terms of compressive strength, fluidity, setting time, and expansion rate was achieved when factor A was 90 g, B was 80 g, C was 0.8 g, and D was 7.5 g. Design Expert was used for solving the model's optimal objective values to further optimize the results of the interaction factor analysis. Compressive strength, fluidity, and expansion rate were set to maximum conditions, and setting time was set to an intermediate horizontal value of 65 min to ensure that the slurry had enough time to be injected into the borehole. Optimization was used to solve the regression model, and the optimal proportions of A, B, C, and D were determined to be 90, 75.7, 0.98, and 4.37 g, respectively. At this point, the desirability value of the model solution is 0.75, indicating that the reliability of the predicted value of the model solution is high.

The optimized proportioning results of the RSM model solution were further validated. The optimized proportions of A = 90 g, B = 75.7 g, C = 0.98 g, and D = 4.37 g were used as the test conditions for the experimental determinations. The measured compressive strength, fluidity, setting time, and expansion rate of the material are 10.5 MPa, 236 mm, 62 min, and 13.5%, respectively, and the predicted values of the model are 10.2 MPa, 229.82 mm, 65 min, and 12.4%, respectively. The errors for each parameter are 2.8%, 2.6%, 4.4%, and 4.8%, and

the error between the predicted and measured values is less than 5%. This small error indicates that the regression model has a good fitting effect and proves the accuracy and adaptability of RSM in optimizing the performance test design of DC materials. The optimal proportions, when converted into percentages, are as follows: A = 52.6%, B = 44.3%, C = 0.6%, and D = 2.5%.

5 Conclusion

Design Expert 11.0 software was used to optimize the orthogonal experimental design of RSM for DC materials, and quadratic multivariate regression equations were established to determine the relationship between the influencing factors of the materials and their performance indexes. The regression model showed high credibility and accuracy and could accurately predict the test results in the test range. It is expected to provide reasonable theoretical guidance for the preparation of DC materials in practical engineering.

ANOVA and RSM analysis revealed that the order of the effects on compressive strength was as follows: binder > expansive agent > drilling cuttings. Drilling cuttings and binder interactions had the greatest degree of influence. The order of effects on fluidity was as follows: drilling cuttings > binder > expansive agent, with the interaction between the drilling cuttings and the coagulant exerting the greatest degree of influence. The order of effects on setting time was coagulant > binder, with drilling cuttings and coagulant having the greatest influence. Meanwhile, the order of effects on expansion rate was as follows: expansive agent > binder > drilling cuttings > coagulant, with the interaction between the expansive agent and binder having the greatest degree of influence.

The sealing characteristics of the DC material were investigated through a simulation of the grouting process, and the microstructure of the material was analyzed. The experimental results verified the feasibility of sealing with this material. The optimal setting of 52.6% drilling cutting, 44.3% binder, 0.6% coagulant, and 2.5% expansive agent was obtained after optimizing the material properties, and the error between the predicted and measured values of the material properties under the optimal setting was less than 5%. The comprehensive performance was superior, which verifies the accuracy and applicability of RSM in optimizing the performance of DC materials.

Data availability statement

The original contributions presented in the study are included in the article/Supplementary Material, further inquiries can be directed to the corresponding author.

Author contributions

XL: Conceptualization, Investigation, Writing–original draft. GH: Funding acquisition, Software, Writing–original draft. YW: Investigation, Writing–original draft. JX: Conceptualization, Methodology, Writing–original draft. JD: Data curation, Supervision, Writing–original draft. BY: Investigation, Validation, Writing–review and editing. MZ: Investigation, Methodology, Writing–review and editing. TL: Resources, Writing–review and editing. BL: Funding acquisition, Supervision, Writing–review and editing. JZ: Data curation, Software, Writing–review and editing.

Funding

Conflict of interest

Authors XL, GH, YW, JX, JD, BY, MZ, and TL were employed by Shanxi Coking Coal Group Co., Ltd.

The remaining authors declare that the research was conducted in the absence of any commercial or financial relationships that could be construed as a potential conflict of interest.

Publisher's note

All claims expressed in this article are solely those of the authors and do not necessarily represent those of their affiliated organizations, or those of the publisher, the editors and the reviewers. Any product that may be evaluated in this article, or claim that may be made by its manufacturer, is not guaranteed or endorsed by the publisher.

References

Bai, B., Rao, D., Chang, T., and Guo, Z. (2019). A nonlinear attachment-detachment model with adsorption hysteresis for suspension-colloidal transport in porous media. *J. Hydrology* 578, 124080. doi:10.1016/j.jhydrol.2019.124080

Bai, B., Zhou, R., Cai, G., Hu, W., and Yang, G. (2021). Coupled thermo-hydromechanical mechanism in view of the soil particle rearrangement of granular thermodynamics. *Comput. Geotechnics* 137, 104272. doi:10.1016/j.compgeo.2021.104272

Chen, K., Wu, D., Zhang, Z., Pan, C., Shen, X., Xia, L., et al. (2022). Modeling and optimization of fly ash–slag-based geopolymer using response surface method and its application in soft soil stabilization. *Constr. Build. Mater.* 315, 125723. doi:10.1016/j.conbuildmat.2021.125723

Fu, J., Wang, D., Li, X., Wang, Z., Shang, Z., Jiang, Z., et al. (2021). Experimental study on the cement-based materials used in coal mine gas extraction for hole sealing. *ACS omega* 6, 21094–21103. doi:10.1021/acsomega.1c02911

Guo, L., Zhou, M., Wang, X., Li, C., and Jia, H. (2022). Preparation of coal gangue-slag-fly ash geopolymer grouting materials. *Constr. Build. Mater.* 328, 126997. doi:10.1016/j.conbuildmat.2022.126997

Jing, M., Ni, G., Xu, Y., Wang, H., Li, Z., and Wang, Z. (2022). Modeling and optimization of mechanical properties of drilling sealing materials based on response surface method. *J. Clean. Prod.* 377, 134452. doi:10.1016/j.jclepro.2022.134452

Li, H., Li, X., Fu, J., Zhu, N., Chen, D., Wang, Y., et al. (2023). Experimental study on compressive behavior and failure characteristics of imitation steel fiber concrete under uniaxial load. *Constr. Build. Mater.* 399, 132599. doi:10.1016/j.conbuildmat.2023.132599

Li, J., Liu, Y., Li, S., and Song, Y. (2022). Experimental investigation of synchronous grouting material prepared with different mineral admixtures. *Materials* 15, 1260. doi:10.3390/ma15031260

Li, S., Zhang, J., Li, Z., Gao, Y., Qi, Y., Li, H., et al. (2019b). Investigation and practical application of a new cementitious anti-washout grouting material. *Constr. Build. Mater.* 224, 66–77. doi:10.1016/j.conbuildmat.2019.07.057

Li, S., Zhang, Q., Liu, B., and Tian, H. (2019a). Research on Tiangu sealing material and sealing technique for gas extraction borehole. *Min. Saf. Environ. Prot.* 46, 44–47.

Liu, H., Li, X., and Yu, Z. (2023b). Influence of hole diameter on mechanical properties and stability of granite rock surrounding tunnels. *Phys. Fluids* 35, 064121.

Liu, S., and Li, X. (2023). Experimental study on the effect of cold soaking with liquid nitrogen on the coal chemical and microstructural characteristics. *Environ. Sci. Pollut. Res.* 30, 36080–36097. doi:10.1007/s11356-022-24821-9

Liu, S., Sun, H., Zhang, D., Yang, K., Li, X., Wang, D., et al. (2023a). Experimental study of effect of liquid nitrogen cold soaking on coal pore structure and fractal characteristics. *Energy* 275, 127470. doi:10.1016/j.energy.2023.127470

Martin, D., Aparicio, P., and Galan, E. (2019). Time evolution of the mineral carbonation of ceramic bricks in a simulated pilot plant using a common clay as sealing material at superficial conditions. *Appl. clay Sci.* 180, 105191. doi:10.1016/j.clay.2019.105191

Ni, G., Dong, K., Li, S., Sun, Q., Huang, D., Wang, N., et al. (2020). Development and performance testing of the new sealing material for gas drainage drilling in coal mine. *Powder Technol.* 363, 152–160. doi:10.1016/j.powtec.2019.12.031

Wang, H., Zhang, B., Yuan, L., Wang, S., Yu, G., and Liu, Z. (2022). Analysis of precursor information for coal and gas outbursts induced by roadway tunneling: a simulation test study for the whole process. *Tunn. Undergr. Space Technol.* 122, 104349. doi:10.1016/j.tust.2021.104349

Wang, Y. (2021). The path of solving environmental pollution problems in mine construction. *Coal Chem. Industry* 44, 107–109.

Wei, Z., Yang, K., He, X., Zhang, J., and Hu, G. (2022). Experimental study on the optimization of coal-based solid waste filling slurry ratio based on the response surface method. *Materials* 15, 5318. doi:10.3390/ma15155318

Xie, H. (2019). Research review of the state key research development program of China: deep rock mechanics and mining theory. *J. China Coal Soc.* 44, 1283–1305. doi:10.13225/j.cnki.jccs.2019.6038

Xiong, L., Zhang, Z., Wan, Z., Zhang, Y., Wang, Z., and Lv, J. (2021). Optimization of grouting material mixture ratio based on multi-objective optimization and multi-attribute decision-making. *Sustainability* 14, 399. doi:10.3390/su14010399

Xiong, W. (2020). Study on repair technology of gas leakage failure borehole of gas extraction. *Min. Saf. Environ. Prot.* 47, 80–83. doi:10.19835/j.issn.1008-4495.2020.01.017

Xue, C., Zhang, L., Wei, J., Zhang, Y., and Xu, L. (2020). Tests on impact resistance of modified cement-based sealing material for mine. *J. Saf. Sci. Technol.* 16, 70–75.

Yan, W., and Chen, B. (2021). Research progress of gas drainage boreholes sealing materials and matching technology in underground coal mine. *Saf. Coal Mines* 52, 175–181. doi:10.13347/j.cnki.mkaq.2021.08.031

Zhang, J., Li, X., Qin, Q., Wang, Y., and Gao, X. (2023). Study on overlying strata movement patterns and mechanisms in super-large mining height stopes. *Bull. Eng. Geol. Environ.* 82, 142. doi:10.1007/s10064-023-03185-5

Zhang, J., Sun, Y., Sun, Z., Wang, Z., Zhao, Y., and Sun, B. (2019). Analysis of macroscopic mechanical properties and mechanism of coal dust/polymer composite grouting material. *Chin. J. Rock Mech. Eng.* 38, 2889–2897.

Zhang, L., and Zhai, J. (2019). Mixture ratio optimization of alkali-activated cement mortar based on response surface method. *Bull. Chin. Ceram. Soc.* 38, 3619–3624. doi:10.16552/j.cnki.issn1001-1625.2019.11.037

Zheng, G., Huang, J., Diao, Y., Ma, A., Su, Y., and Chen, H. (2021). Formulation and performance of slow-setting cement-based grouting paste (SCGP) for capsule grouting technology using orthogonal test. *Constr. Build. Mater.* 302, 124204. doi:10.1016/j.conbuildmat.2021.124204

Zhu, L., Jin, Z., Zhao, Y., and Duan, Y. (2021). Rheological properties of cemented coal gangue backfill based on response surface methodology. *Constr. Build. Mater.* 306, 124836. doi:10.1016/j.conbuildmat.2021.124836

Zuo, N., Zhao, J., Shi, Z., Wang, X., Wang, P., and Wang, W. (2022). Study on preparation and properties of quick-setting low-cost sealing materials. *Energy Chem. Ind.* 43, 19–23.